Polyoxoanion Coordination Chemistry: Synthesis and Characterization of the Heterometallic, Hexanuclear Clusters [{Zn(bipy)$_2$}$_2$V$_4$O$_{12}$], [{Zn(phen)$_2$}$_2$V$_4$O$_{12}$]·H$_2$O, and [{Ni(bipy)$_2$}$_2$Mo$_4$O$_{14}$]

Yiping Zhang,[†] Pamela J. Zapf,[‡] Linda M. Meyer,[†] Robert C. Haushalter,*,[†] and Jon Zubieta*,[‡]

NEC Research Institute, 4 Independence Way, Princeton, New Jersey 08540, and Department of Chemistry, Syracuse University, Syracuse, New York 13244

The hydrothermal reactions of vanadium oxide and molybdenum oxide starting materials with divalent first-row transition metal cations in the presence of nitrogen donor chelating ligands yield the heterometallic hexanuclear clusters [{Zn(bipy)$_2$}$_2$V$_4$O$_{12}$] (**2**), [{Zn(phen)$_2$}$_2$V$_4$O$_{12}$]·H$_2$O (**3**·H$_2$O), and [{Ni(bipy)$_2$}$_2$Mo$_4$O$_{14}$] (**4**). A similar reaction in the presence of excess 2,2′-bipyridine yields [Zn(bipy)$_3$]$_2$[V$_4$O$_{12}$]·11H$_2$O (**1**·11H$_2$O), a species with an isolated {V$_4$O$_{12}$}$^{4-}$ cluster. The structure of **2** consists of a {V$_4$O$_{12}$}$^{4-}$ ring covalently attached to each of two {Zn(bipy)$_2$}$^{2+}$ moieties through the terminal oxo groups of alternate vanadium sites. In contrast, the structure of **3** exhibits a {V$_4$O$_{12}$}$^{4-}$ ring linked through oxo groups of adjacent vanadium sites to two {Zn(phen)$_2$}$^{2+}$ moieties. The structure of **4** is constructed from two {Mo$_2$O$_7$}$^{2-}$ units linked through two {Ni(bipy)$_2$}$^{2+}$ groups to form a cyclic 12-membered {Mo$_4$Ni$_2$O$_6$} core. Crystal data: [Zn(bipy)$_3$]$_2$[V$_4$O$_{12}$]·11H$_2$O (**1**·11H$_2$O), a = 21.910(4) Å, b = 14.044(2) Å, c = 23.815(4) Å, β = 106.15(1)°, monoclinic, $C2/c$, Z = 4; [{Zn(bipy)$_2$}$_2$V$_4$O$_{12}$] (**2**), a = 12.017(2) Å, c = 15.120(2) Å, tetragonal $P4_2/n$, Z = 2. [{Zn(o-phen)$_2$}$_2$V$_4$O$_{12}$]·H$_2$O (**3**·H$_2$O), a = 18.182(2) Å, b = 11.3668(9) Å, c = 23.455(2) Å, β = 97.815(7)°, monoclinic $P2_1/c$, Z = 4; [{Ni(bipy)$_2${$_2$Mo$_4$O$_{14}$] (**4**), a = 12.323(2) Å, c = 14.897(4) Å, tetragonal $P4_22_12$, Z = 2.

Introduction

Polyoxoanions constitute an enormous class of compounds whose unusual structural versatility and reactivity affords practical applications to catalysis, biology, medicine, and materials science.[1−3] While the polyanion surface is populated by weakly basic oxo groups which render such clusters relatively unreactive toward substitution or polymerization reactions, the past decade has witnessed significant growth of the coordination chemistry of polyoxoanions. This activity has resulted in the development of two major subclasses of polyoxoanions: clusters incorporating conventional ligands[4] and clusters supporting organometallic fragments.[5] The latter subgroup is represented among others by structures based on the tetrametalate core, such as {[η-C$_8$H$_{12}$)Ir]$_2$(V$_4$O$_{12}$)}$^{2-}$,[6] on the hexametalate unit, such as [M(CO)$_3$(Nb$_2$W$_4$O$_{19}$)]$^{3-}$,[7] [(C$_5$H$_5$)Rh]$_4$(V$_6$O$_{19}$),[8,9] and {[(C$_8$-H$_{12}$)Ir]$_5$(Nb$_2$W$_4$O$_{19}$)}$^{3-}$,[10] on the ε-Keggin core, as in [(C$_5$Me$_5$)-Rh(Mo$_{13}$O$_{40}$)]$^{2+}$,[11] and on the Dawson cluster core, exemplified by [(COD)IrW$_{15}$Nb$_3$P$_2$O$_{62}$]$^{8-}$[12] and [(C$_5$H$_5$)TiW$_{15}$V$_3$P$_2$-O$_{62}$]$^{6-}$.[13]

In contrast to the emerging chemistry of the polyanion-supported organometallic class of clusters, the coordination chemistry of polyanions with classical coordination complexes and fragments remains generally undeveloped. However, recent developments in the chemistry of metal oxide solid phases have demonstrated that transition metal coordination complexes may act as covalently bound subunits of the metal oxide framework itself, as described for [Cu(en)$_2$V$_2$O$_6$][14] or may serve as inorganic bridging "ligands", linking polyanion clusters into one- and two-dimensional networks, as shown for [Cu(en)$_2$]$_3$[V$_{15}$O$_{36}$Cl] and {[Ni(en)$_2$]$_3$[V$_{18}$O$_{42}$Cl]}$^{0.5-}$.[15] It is noteworthy that these solid state/coordination complex materials may be isolated only in the hydrothermal domain, suggesting that the enhanced solubility and crystal growth properties are crucial to the syntheses. This observation suggested that suitable modification of the synthetic parameters of the hydrothermal domain should afford polyoxoanion/coordination complex clusters as molecular analogues of the solid phases. This expectation has been realized in the isolation of [{Zn(bipy)$_2$}$_2$V$_4$O$_{12}$] (**2**), [{Zn(phen)$_2$}$_2$V$_4$O$_{12}$]·H$_2$O (**3**·H$_2$O), and [{Ni(bipy)$_2$}$_2$Mo$_4$O$_{14}$] (**4**). The influence of reaction stoichiometries and other conditions is evident in the preparation of [Zn(bipy)$_3$]$_2$[V$_4$O$_{12}$]·11H$_2$O (**1**·11H$_2$O) in which the complex cation [Zn(bipy)$_3$]$^{2+}$ serves as a charge-compensating unit and does not form a covalent attachment to the isolated [V$_4$O$_{12}$]$^{4-}$ polyanion.

Experimental Section

Reagents were purchased from Aldrich Chemical Co. and used without further purification. All of the syntheses were carried out in

† NEC.

‡ Syracuse University.

⊗ Abstract published in *Advance ACS Abstracts,* April 15, 1997.

(1) Pope, M. T. *Heteropoly and Isopoly Oxometalates*; Springer-Verlag: New York, 1983.

(2) Pope, M. T.; Müller, A. *Angew. Chem., Int. Ed. Engl.* **1991**, *30*, 34.

(3) Pope, M. T.; Müller, A. *Polyoxometalates: From Platonic Solids to Antiretroviral Activity*; Kluwer Academic Press: Dordrecht, The Netherlands, 1994.

(4) Khan, M. I.; Zubieta, J. *Prog. Inorg. Chem.* **1995**, *43*, 1.

(5) Day, V. W.; Klemperer, W. G. In *Polyoxometalates: From Platonic Solids to Antiretroviral Activity*; Pope, M. T., Müller, A., Eds.; Kluwer Academic Press: Dordrecht, The Netherlands, 1994, p. 87.

(6) Day, V. W.; Klemperer, W. G.; Yagasaki, A. *Chem. Lett.* **1990**, 1267.

(7) Besecher, C. J.; Day, V. W.; Klemperer, W. G.; Thompson, M. R. *Inorg. Chem.* **1985**, *24*, 44.

(8) Chae, H. K.; Klemperer, W. G. *Inorg. Chem.* **1989**, *28*, 1424.

(9) Hayashi, Y.; Ozawa, Y.; Isobe, K. *Inorg. Chem.* **1991**, *30*, 1025.

(10) Day, V. W.; Klemperer, W. G.; Main, D. J. *Inorg. Chem.* **1990**, *29*, 2345.

(11) Chae, H. K.; Klemperer, W. B.; Páez Loyo, D. E.; Day, V. W.; Eberspacher, T. A. *Inorg. Chem.* **1992**, *31*, 3187.

(12) Pohl, M.; Lyon, D. K.; Miguno, N.; Nomiya, K.; Finke, R. G. *Inorg. Chem.* **1995**, *34*, 1413.

(13) Rapko, B. M.; Pohl, M.; Finke, R. G. *Inorg. Chem.* **1994**, *33*, 3625.

(14) DeBord, J. R. D.; Zhang, Y.; Haushalter, R. C.; Zubieta, J.; O'Connor, C. J. *J. Solid State Chem.* **1996**, in press.

(15) DeBord, J. R. D.; Haushalter, R. C.; Rose, D. J.; Zapf, P. J.; Zubieta, J. Unpublished results.

Table 1. Crystallographic Data for the Structural Studies of [Zn(bipy)$_3$]$_2$[V$_4$O$_{12}$]·11H$_2$O (**1**·11H$_2$O), [{Zn(bipy)$_2$}$_2$V$_4$O$_{12}$] (**2**), [{Zn(phen)$_2$}$_2$V$_4$O$_{12}$]·H$_2$O (**3**·H$_2$O) and [{Ni(bipy)$_2$}$_2$Mo$_4$O$_{14}$] (**4**)

	1·11H$_2$O	**2**	**3**·H$_2$O	**4**
chem formula	C$_{60}$H$_{70}$N$_{12}$ O$_{23}$V$_4$Zn$_2$	C$_{40}$H$_{32}$N$_8$ O$_{12}$V$_4$Zn$_2$	C$_{48}$H$_{34}$N$_8$ O$_{13}$V$_4$Zn$_2$	C$_{40}$H$_{32}$N$_8$ O$_{14}$Ni$_2$Mo$_4$
a, Å	21.910(4)	12.017(2)	18.182(2)	12.323(2)
b, Å	14.044(2)		11.3668(9)	
c, Å	23.815(4)	15.120(2)	23.455(2)	14.897(3)
β, deg	106.15(1)		97.815(7)	
V, Å^3	7038(1)	2183.7(7)	4802.4(7)	2262.2(11)
Z	4	2	4	2
fw	1661.81	1151.27	1265.40	1349.89
space group	*C*2/*c*	*P*4$_2$/*n*	*P*2$_1$/*c*	*P*4$_2$2$_1$2
T, °C	20 ± 1	20 ± 1	20 ± 1	20 ± 1
λ, Å	0.710 73	0.710 73	0.710 73	0.710 73
D_{calc}, g cm^{-3}	1.568	1.751	1.750	1.982
D_{obs}, g cm^{-3}	1.59(2)	1.73(2)	1.77(2)	2.01(2)
μ, cm^{-1}	12.63	19.73	18.09	19.65
R^a	0.052	0.034	0.032	0.061
$R_w{}^b$	0.064	0.037	0.036	0.063

^{a} $R = \sum||F_o| - |F_c||/\sum|F_o|$. ^{b} $R_w = [\sum w(|F_o| - |F_c|)^2/\sum w|F_o|^2]^{1/2}$.

polytetrafluoroethylene-lined stainless steel containers under autogenous pressure. The reactants were stirred briefly before heating. The 23 mL reaction vessels were filled to approximately 40% volume capacity. Compounds **1**–**3** are diamagnetic, while compound **4** exhibits a room-temperature magnetism μ_{eff} of 3.21 μ_B.

Synthesis. [Zn(2,2′-bipy)$_3$]$_2$[V$_4$O$_{12}$]·11H$_2$O (1·11H$_2$O). A mixture of V$_2$O$_5$ (0.087 g), ZnO (0.049 g), 2,2′-bipyridine (0.158 g), and H$_2$O in the mole ratio 1.0:1.26:2.12:1162 was heated at 170 °C for 68 h. The reaction vessel was found to contain a mixture of light pink plates of **1**·11H$_2$O and black rods of [VO(VO$_3$)$_6${VO(2,2′-bipy)$_2$}$_2$],[16] which were separated mechanically. The yield of **1**·11H$_2$O was *ca.* 30% based on vanadium. Anal. Calcd for C$_{60}$H$_{92}$N$_{12}$O$_{23}$V$_4$Zn$_2$: C, 42.8; H, 5.51; N, 9.98. Found: C, 42.5; H, 5.32; N, 9.89.

[{Zn(2,2′-bipy)$_2$}$_2$V$_4$O$_{12}$] (2). A mixture of V$_2$O$_5$ (0.142 g), ZnO (0.093 g), 2,2′-bipyridine (0.156 g), and H$_2$O in the mole ratio 1.0:1.46:1.28:711 was heated at 170 °C for 68 h, yielding white rods of **2** as a minor phase, with brown blocks of [{Zn(2,2′-bipy)$_2$}$_2$V$_6$O$_{17}$][17] constituting the major product. Attempts to optimize the synthesis of **2** proved unsuccessful.

[{Zn(o-phen)$_2$}$_2$V$_4$O$_{12}$]·H$_2$O (3·H$_2$O). A mixture of V$_2$O$_5$ (0.168 g), ZnO (0.184 g), 1,10-phenanthroline (0.304 g), and H$_2$O in the mole ratio 1.0:2.45:1.83:601 was heated at 200 °C for 47 h, yielding pink plates of **3**·H$_2$O in *ca.* 30% yield, contaminated by a small amount of unreacted ZnO. Attempts to prepare **3** as a monophasic material were unsuccessful.

[{Ni(2,2′-bipy)$_2$}$_2$Mo$_4$O$_{14}$] (4). A mixture of Na$_2$MoO$_3$ (1.33 g), MoO$_3$ (0.801 g), 2,2′-bipyridine (1.45 g), NiCl$_2$ (Alfa Aesar, 1.097 g), and H$_2$O (5.129 g) in the mole ratio 1:1:1.68:0.84:51.9 was heated at 160 °C for 46 h in a sealed borosilicate ampule of 22 mL volume. Large amethyst blocks of **4** were separated from a pale green paste by flotation in water. Anal. Calcd for C$_{40}$H$_{32}$N$_8$O$_{14}$Ni$_2$Mo$_4$: C, 35.6; H, 2.37; N, 8.30. Found: C, 35.8; H, 2.19; N, 8.21.

X-ray Crystallography. Structural measurements for compounds **1**–**3** were performed on a Rigaku AFC7R diffractometer, while data for **4** were collected on a Rigaku AFC5S diffractometer. In all cases, graphite-monochromated MoK$_\alpha$ radiation (λ(MoK$_\alpha$) = 0.710 73 Å) was used.

The data for **1**–**3** were collected at a temperature of 20 ± 1 °C using the ω−2θ scan technique to 40.1, 55.1, and 50.1° in 2θ, respectively, at scan speeds of 16, 32, and 16.0°/min in ω, respectively. In the case of **4**, similar conditions were employed but with the 2θ maximum of 45° and a variable scan speed of 4−8°/min in ω. The intensities of three standard reflections measured after every 150 reflections remained constant throughout the data collections. An empirical absorption correction using the program DIFABS was applied

to data[18] for **1**–**3**, while in the case of **4** an empirical absorption correction based on φ scans was used. The data were corrected for Lorentz and polarization effects. The structures were solved by direct methods.[19] Metal and oxygen atoms were refined anisotropically for **1** and **4**; all non-hydrogen atoms were refined anisotropically for **2** and **3**. Neutral atom scattering factors were taken from Cromer and Waber,[20] and anomalous dispersion corrections were taken from those of Creagh and McAuley.[21] All calculations were performed using the SHELXTL[22 a] or teXsan[22b] crystallographic software packages. In the case of compound **4**, the absolute configuration was determined from the Flack x parameter, calculated for each configuration.[23]

Crystallographic date for **1**–**4** are listed in Table 1. Atomic positional parameters and isotropic temperature factors for **1**–**4** are given in Tables 2–5, respectively. Selected bond lengths and angles for **1**–**4** are listed in Tables 6–9, respectively. ORTEP figures for the cation of **1** and for **2** and **3** are provided in the Supporting Information as Figures S1–3, respectively.

Results and Discussion

The isolation of compounds **1**–**4** relies on hydrothermal techniques of synthesis.[24−27] By the employment of temperatures in the 120−270 °C range under autogenous pressures, rather than the high-temperature methods now routinely used in solid-state chemistry, "self-assembly" of metastable phases which retain the bond relationships between most of the constituent atoms may be accomplished from simple molecular precursors. A variety of starting materials may be introduced since most species are soluble under these conditions of synthesis. However, since the method of synthesis depends on "self-assembly" of the products from the molecular precursors, the elements of mechanistic control are generally absent and the identity of the products under a given set of conditions is often unpredictable. On the other hand, the very vastness of

(16) Huan, G.; Johnson, J. W.; Jacobson, A. J.; Merola, J. S. *J. Solid State Chem.* **1991**, *91*, 385.
(17) Zhang, Y.; DeBord, J. R. D.; Haushalter, R. C.; Clearfield, A.; Zubieta, J.; O'Connor, C. J. *Angew. Chem., Int. Ed. Engl.* **1996**, in press.
(18) Walker, N.; Stuart, D. *Acta Crystallogr., Sect. A* **1983**, *39*, 158.
(19) teXsan: Texray Structural Analysis Package (revised), Molecular Structure Corp., The Woodlands, TX, 1992.
(20) Cromer, D. T.; Waber, J. T. *International Tables for X-Ray Crystallography*; Kynoch Press: Birmingham, England, 1974; Vol. IV.
(21) Creagh, D. C.; McAuley, J. W. J. *International Tables for X-Ray Crystallography*; Kluwer Academic, Boston, MA, 1992; Vol. C, Table 4,.2. 6. 8.
(22) (a) SHELXTL PC Siemens Analytical X-Ray Instruments, Inc., Madison, WI, 1990. (b) *teXsan*: Crystal Structure Analysis Package, Molecular Structure Corp., The Woodlands, TX, 1985, 1992.
(23) Flack, H. D.; Bernardinelli, G. *Acta Crystallogr.* **1985**, *A41*, 500. Flack, H. D. *Acta Crystallogr.* **1985**, *A39*, 87.
(24) Figlarz, M. *Chem. Scr.* **1988**, *28*, 3.
(25) Rouxel, J. *Chim. Scr.* **1988**, *28*, 33.
(26) Laudise, R. A. *Chem. Eng. News* **1987**, Sept. 8, 30.
(27) Gopalakrishnan, J. *Chem. Mater.* **1995**, *7*, 1265.

Table 2. Atomic Positional Parameters and Isotropic Temperature Factors ($\mathring{A}^2$) or [Zn(bipy)$_3$}]$_2$[V$_4$O$_{12}$]·11H$_2$O (**1**·11H$_2$O)

atom	x	y	z	$B_{eq}{}^a$
Zn(1)	0.83221(5)	0.46457(8)	0.73328(5)	2.56(3)
V(1)	0.57672(8)	0.3716(1)	0.50454(7)	2.67(4)
V(2)	0.53736(8)	0.5673(1)	0.42437(7)	2.66(4)
O(1)	0.5613(4)	0.2609(5)	0.4849(3)	4.4(2)
O(2)	0.6526(3)	0.3803(5)	0.5366(3)	4.4(2)
O(3)	0.5333(3)	0.4054(5)	0.5548(3)	3.7(2)
O(4)	0.5547(3)	0.4448(4)	0.4398(3)	3.3(2)
O(5)	0.5239(3)	0.5864(5)	0.3544(3)	3.9(2)
O(6)	0.5961(3)	0.6362(5)	0.4606(3)	4.1(2)
O(7)	0.6391(4)	0.1049(6)	0.5028(4)	6.8(2)
O(8)	0.5000	0.4893(7)	0.2500	4.3(2)
O(9)	0.7509(5)	0.4718(7)	0.5064(4)	7.7(2)
O(10)	0.7247(4)	0.6640(6)	0.5096(4)	5.9(2)
O(11)	0.5695(4)	0.7835(6)	0.5324(3)	5.5(2)
O(12)	0.9400(4)	0.4827(6)	0.9591(4)	6.4(2)
N(1)	0.7388(4)	0.5155(5)	0.6915(3)	2.5(2)
N(2)	0.7754(4)	0.4120(5)	0.7896(3)	2.9(2)
N(3)	0.8238(4)	0.3346(5)	0.6828(3)	2.6(2)
N(4)	0.9131(3)	0.3834(5)	0.7790(3)	2.5(2)
N(5)	0.8780(4)	0.5474(5)	0.6809(3)	2.6(2)
N(6)	0.8601(4)	0.5942(5)	0.7831(3)	2.7(2)
C(1)	0.7234(5)	0.5637(7)	0.6404(4)	3.2(2)
C(2)	0.6605(5)	0.5901(7)	0.6132(4)	3.6(2)
C(3)	0.6136(5)	0.5669(7)	0.6391(4)	3.7(2)
C(4)	0.6300(5)	0.5177(7)	0.6925(5)	3.6(2)
C(5)	0.6930(5)	0.4944(6)	0.7175(4)	2.6(2)
C(6)	0.7151(5)	0.4422(7)	0.7741(4)	2.7(2)
C(7)	0.6735(5)	0.4250(7)	0.8084(5)	3.7(2)
C(8)	0.6976(6)	0.3743(8)	0.8610(5)	4.7(3)
C(9)	0.7598(5)	0.3415(8)	0.8762(5)	4.5(3)
C(10)	0.7988(5)	0.3615(7)	0.8395(5)	3.6(2)
C(11)	0.7792(5)	0.3189(7)	0.6302(4)	3.4(2)
C(12)	0.7793(5)	0.2341(8)	0.6002(5)	4.0(2)
C(13)	0.8246(5)	0.1637(8)	0.6235(5)	4.2(2)
C(14)	0.8697(5)	0.1804(7)	0.6786(4)	3.5(2)
C(15)	0.8672(4)	0.2679(6)	0.7054(4)	2.4(2)
C(16)	0.9143(4)	0.2926(7)	0.7620(4)	2.5(2)
C(17)	0.9560(4)	0.2248(7)	0.7943(4)	2.9(2)
C(18)	0.9982(5)	0.2541(7)	0.8480(4)	3.3(2)
C(19)	0.9980(5)	0.3480(7)	0.8648(4)	3.3(2)
C(20)	0.9546(5)	0.4116(7)	0.8298(4)	3.2(2)
C(21)	0.8852(5)	0.5177(7)	0.6291(4)	3.3(2)
C(22)	0.9159(5)	0.5748(8)	0.5970(5)	4.3(3)
C(23)	0.9392(6)	0.6647(9)	0.6198(5)	5.1(3)
C(24)	0.9299(5)	0.6963(8)	0.6723(5)	4.4(3)
C(25)	0.8986(5)	0.6334(7)	0.7013(4)	2.9(2)
C(26)	0.8885(5)	0.6612(7)	0.7587(4)	2.9(2)
C(27)	0.9061(5)	0.7504(7)	0.7843(5)	3.7(2)
C(28)	0.8952(5)	0.7696(8)	0.8382(5)	4.5(3)
C(29)	0.8662(5)	0.7005(8)	0.8642(5)	4.1(2)
C(30)	0.8493(5)	0.6134(7)	0.8360(5)	3.7(2)

^{a} $B_{eq} = {}^8/_3\pi^2(U_{11}(aa^*)^2 + U_{22}(bb^*)^2 + U_{33}(cc^*)^2 + 2U_{12}aa^*bb^* \cos \gamma + 2U_{13}aa^*cc^* \cos \beta + 2U_{23}bb^*cc^* \cos \alpha.$

Table 3. Atomic Positional Parameters and Isotropic Temperature Factors ($\mathring{A}^2$) for [{Zn(bipy)$_2$}$_2$V$_4$O$_{12}$] (**2**)

atom	x	y	z	B_{eq}
Zn(1)	0.2500	0.2500	0.50295(4)	2.92(1)
V(1)	0.22381(5)	0.41919(5)	0.69607(4)	2.62(1)
O(1)	0.2149(2)	0.3743(3)	0.5940(2)	4.48(8)
O(2)	0.2107(2)	0.5523(2)	0.6975(2)	4.73(8)
O(3)	0.3594(2)	0.3846(3)	0.7385(2)	4.75(8)
N(1)	0.2418(3)	0.3845(3)	0.4020(2)	3.22(8)
N(2)	0.4150(2)	0.2968(3)	0.4855(2)	2.99(7)
C(1)	0.4967(3)	0.2479(4)	0.5310(3)	3.79(10)
C(2)	0.6064(4)	0.2769(4)	0.5178(3)	5.0(1)
C(3)	0.6318(4)	0.3582(4)	0.4571(3)	5.0(1)
C(4)	0.5480(4)	0.4095(4)	0.4126(3)	4.1(1)
C(5)	0.4383(3)	0.3766(3)	0.4270(3)	3.09(9)
C(6)	0.3413(3)	0.4284(3)	0.3820(3)	3.10(8)
C(7)	0.3511(4)	0.5190(4)	0.3249(3)	4.2(1)
C(8)	0.2555(4)	0.5671(4)	0.2912(3)	4.7(1)
C(9)	0.1531(4)	0.5245(4)	0.3141(3)	4.5(1)
C(10)	0.1506(4)	0.4327(4)	0.3690(3)	4.1(1)

120 h), a mixture of NiCl$_2$·6H$_2$O, CsVO$_3$, vanadium metal, and ethylenediamine yields Cs$_{0.5}$[Ni(en)$_2$]$_3$[V$_{18}$O$_{42}$Cl], a two-dimensional solid constructed from {V$_{18}$O$_{42}$Cl}$^{n-}$ clusters covalently bridged through {Ni(en)$_2$}$^{2+}$ fragments.[15] By the adoption conditions similar to those employed for the synthesis of [{Zn(bipy)$_2$}$_2$V$_6$O$_{17}$], with minor variations in reaction times and stoichiometries, the molecular clusters of the study **1−4** were isolated.

Within the group of vanadium oxide based clusters **1−3**, the influence of synthetic conditions is noteworthy. Thus, increasing the ratio of 2,2′-bipyridine to V$_2$O$_5$ results in the formation of the tris-chelate cation {Zn(bipy)$_3$}$^{2+}$, which acts as a space-filling and charge-compensating cation for the "naked" vanadium oxide cluster, [V$_4$O$_{12}$]$^{4-}$, found in compound **1**·11H$_2$O. In contrast, reducing the relative concentration of the 2,2′-bipyridine prevents the formation of the tris-chelate, allowing the isolation of the heterometallic, hexanuclear anion cluster [{Zn(bipy)$_2$}$_2$V$_4$O$_{12}$] (**2**). Under similar reaction conditions, but introducing phenanthroline rather than 2,2′-bipyridine, the compositionally similar cluster [{Zn(phen)$_2$}$_2$V$_4$O$_{12}$] (**3**) is formed. However, as noted below, the structure of **3** is quite distinct from that of **2**, suggesting that the steric constraints imposed by the phenanthroline ligand are quite distinct from those of the 2,2′-bipyridine.

Under reaction conditions similar to those employed for **1−3**, the Mo/Ni/O system also yields a heterometallic, hexanuclear species [{Ni(bipy)$_2$}$_2$Mo$_4$O$_{14}$] (**4**). Since molybdenum does not form the analogous {M$_4$O$_{12}$} core associated with the vanadium oxide system, it was not unexpected that **4** should possess a unique composition and structure.

As shown in Figure 1a, the structure of the anion of **1** consists of an isolated molecular cluster, [V$_4$O$_{12}$]$^{4-}$, with a cyclic eight-membered {V$_4$O$_4$} core. The structure of this cluster is essentially identical to that observed in (Bu$_4$N)$_3$HV$_4$O$_{12}$.[28] The vanadium sites exhibit distorted tetrahedral geometry defined by two terminal oxo groups with an average V−O$_t$ bond distance of 1.635(7) Å and two bridging oxo groups with V−O$_b$ of 1.791(7) Å. As illustrated in Figure 1b, the [V$_4$O$_{12}$]$^{4-}$ clusters and {Zn(bipy)$_3$}$^{2+}$ cations form virtual layers separated by water molecules. The anion clusters are strongly hydrogen-bonded to the water molecules, as suggested by the short nonbonded O(cluster)···O(water) contacts listed in Table 6.

It is noteworthy that previously structurally characterized examples of the [V$_4$O$_{12}$]$^{4-}$ core were isolated from nonaqueous

the hydrothermal parameter space—stoichiometries, temperature, pressure, pH, fill volume, starting materials, templates, mineralizers—allows variations in conditions, permitting the isolation of both molecular species and solid-phase materials for similar compositional systems, as previously noted for the oxovanadium−organophosphonate class of compounds.[4] While, *faux de mieux*, the parameter space must be explored without a background of well-developed reaction pathways, a judicious manipulation of reaction conditions can provide a reliable domain for the isolation of classes of materials.

Such general principles may be discerned in the preparation of **1−4**. For example, the hydrothermal reaction of ZnO, 2,2′-bipyridine, and V$_2$O$_5$ at 170 °C for 44 h yields the layered vanadium oxide with an interlayer Zn coordination complex, [{Zn(bipy)$_2$}$_2$V$_6$O$_{17}$].[17] In contrast, under reducing conditions, elevated temperatures, and prolonged reaction times (200 °C,

(28) Fuchs, J.; Mahjour, S.; Pickardt, J. *Angew. Chem., Int. Ed. Engl.* **1976**, *15*, 374.

Table 4. Atomic Positional Parameters and Isotropic Temperature Factors ($Å^2$) or [{Zn(o-phen)$_2$}$_2$V$_4$O$_{12}$]·H$_2$O (**3**·H$_2$O)

atom	x	y	z	B_{eq}
Zn(1)	0.69092(3)	−0.22298(5)	0.15063(2)	2.22(1)
Zn(2)	0.80057(3)	−0.76114(5)	0.37006(2)	2.53(1)
V(1)	0.65539(4)	−0.32323(8)	0.28339(3)	2.45(2)
V(2)	0.66567(4)	−0.51295(7)	0.18536(3)	2.10(2)
V(3)	0.83918(4)	−0.59562(7)	0.25638(3)	2.33(2)
V(4)	0.80186(4)	−0.45333(7)	0.36521(3)	2.46(2)
O(1)	0.5840(2)	−0.2636(3)	0.3058(1)	3.91(9)
O(2)	0.6904(2)	−0.2324(3)	0.2385(1)	2.97(8)
O(3)	0.6240(2)	−0.4541(3)	0.2440(1)	3.10(8)
O(4)	0.6772(2)	−0.4044(3)	0.1405(1)	2.77(8)
O(5)	0.6120(2)	−0.6125(3)	0.1521(1)	3.14(8)
O(6)	0.7530(2)	−0.5779(3)	0.2111(1)	3.60(9)
O(7)	0.9058(2)	−0.6018(3)	0.2174(1)	3.18(8)
O(8)	0.8390(2)	−0.7194(3)	0.2937(1)	2.92(8)
O(9)	0.8546(2)	−0.4747(3)	0.3065(1)	3.07(8)
O(10)	0.7764(2)	−0.5861(3)	0.3862(1)	3.23(8)
O(11)	0.8539(2)	−0.3910(3)	0.4182(1)	4.23(9)
O(12)	0.7233(2)	−0.3627(3)	0.3428(1)	3.34(8)
O(13)	0.7615(5)	0.0531(9)	1.0062(4)	14.5(4)
N(1)	0.6653(2)	−0.2198(3)	0.0577(2)	2.77(9)
N(2)	0.5744(2)	−0.1711(3)	0.1364(2)	2.40(9)
N(3)	0.7273(2)	−0.0408(3)	0.1479(2)	2.50(9)
N(4)	0.8108(2)	−0.2362(3)	0.1613(2)	2.31(9)
N(5)	0.8463(2)	−0.9401(4)	0.3583(2)	2.75(9)
N(6)	0.9088(2)	−0.7576(4)	0.4211(2)	2.80(9)
N(7)	0.6931(2)	−0.8117(3)	0.3316(2)	2.49(9)
N(8)	0.7493(2)	−0.8313(3)	0.4436(2)	2.59(9)
C(1)	0.5934(3)	−0.1993(4)	0.0385(2)	2.9(1)
C(2)	0.5451(3)	−0.1713(4)	0.0798(2)	2.7(1)
C(3)	0.5317(3)	−0.1385(4)	0.1748(2)	3.1(1)
C(4)	0.4578(3)	−0.1043(5)	0.1597(3)	3.9(1)
C(5)	0.4267(3)	−0.1081(5)	0.1036(3)	4.4(1)
C(6)	0.4703(3)	−0.1427(5)	0.0616(2)	3.8(1)
C(7)	0.4425(4)	−0.1508(6)	0.0010(3)	5.6(2)
C(8)	0.4875(4)	−0.1791(7)	0.0369(3)	6.0(2)
C(9)	0.5653(4)	−0.2023(5)	0.0208(2)	4.4(2)
C(10)	0.6161(4)	−0.2264(6)	0.0586(2)	5.6(2)
C(11)	0.6882(4)	−0.2475(6)	0.0389(2)	5.1(2)
C(12)	0.7117(3)	−0.2431(5)	0.0200(2)	3.9(1)
C(13)	0.8459(3)	−0.1306(4)	0.1661(2)	2.4(1)
C(14)	0.8019(3)	−0.0268(4)	0.1576(2)	2.5(1)
C(15)	0.6854(3)	0.0539(4)	0.1371(2)	3.2(1)
C(16)	0.7153(3)	0.1669(4)	0.1355(2)	3.4(1)
C(17)	0.7901(3)	0.1819(4)	0.1475(2)	3.4(1)
C(18)	0.8349(3)	0.0844(4)	0.1593(2)	3.2(1)
C(19)	0.9144(3)	0.0911(5)	0.1729(3)	4.5(2)
C(20)	0.9568(3)	−0.0059(5)	0.1827(3)	4.5(2)
C(21)	0.9236(3)	−0.1202(4)	0.1792(2)	3.2(1)
C(22)	0.9645(3)	−0.2253(5)	0.1901(2)	3.2(1)
C(23)	0.9279(3)	−0.3306(4)	0.1865(2)	3.1(1)
C(24)	0.8508(3)	−0.330(4)	0.1706(2)	2.8(1)
C(25)	0.9162(3)	−0.9541(4)	0.3855(2)	2.7(1)
C(26)	0.9488(3)	−0.8577(4)	0.4190(2)	2.7(1)
C(27)	0.9374(3)	−0.6676(5)	0.4522(2)	4.0(1)
C(28)	1.0086(3)	−0.6731(5)	0.4844(3)	4.8(2)
C(29)	1.0498(3)	−0.7729(6)	0.4822(2)	4.3(1)
C(30)	1.0215(3)	−0.8684(5)	0.4493(2)	3.4(1)
C(31)	1.0606(3)	−0.9761(6)	0.4445(3)	4.4(2)
C(32)	1.0313(3)	−1.0650(5)	0.4115(3)	4.4(2)
C(33)	0.9569(3)	−1.0577(5)	0.3815(2)	3.3(1)
C(34)	0.9232(3)	−1.1493(5)	0.3481(3)	4.3(1)
C(35)	0.8528(3)	−1.1351(5)	0.3205(2)	4.0(1)
C(36)	0.8157(3)	−1.0293(5)	0.3261(2)	3.5(1)
C(37)	0.6520(2)	−0.8689(4)	0.3667(2)	2.4(1)
C(38)	0.6820(2)	−0.8801(4)	0.4262(2)	2.4(1)
C(39)	0.7777(3)	−0.8421(5)	0.4988(2)	3.3(1)
C(40)	0.7414(3)	−0.9018(5)	0.5385(2)	3.8(1)
C(41)	0.6727(3)	−0.9514(5)	0.5214(2)	3.7(1)
C(42)	0.6418(3)	−0.9396(4)	0.4638(2)	3.0(1)
C(43)	0.5710(3)	−0.9884(5)	0.4421(3)	4.2(1)
C(44)	0.5426(3)	−0.9772(5)	0.3865(3)	4.3(2)
C(45)	0.5823(3)	−0.9164(5)	0.3469(2)	3.1(1)
C(46)	0.5534(3)	−0.8993(5)	0.2884(2)	3.6(1)
C(47)	0.5946(3)	−0.8381(5)	0.2542(2)	3.8(1)
C(48)	0.6652(3)	−0.7952(5)	0.2771(2)	3.1(1)

Table 5. Atomic Positional Parameters ($\times 10^4$) and Isotropic Temperature Factors ($Å^2 \times 10^3$) for [{Ni(bipy)$_2$}$_2$Mo$_4$O$_{14}$] (**4**)

	x	y	z	U(eq)^a
Mo(1)	5462(2)	2887(2)	777(2)	22(1)
Ni(2)	5000	5000	2365(2)	20(1)
O(1)	4570(13)	2106(13)	185(9)	41(6)
O(2)	6188(14)	2102(14)	1553(11)	41(6)
O(3)	1468(12)	1468(12)	5000	33(6)
O(4)	4711(12)	3861(13)	1352(10)	40(6)
N(1)	3388(12)	5382(13)	2458(11)	19(4)
N(2)	5062(15)	6241(14)	3304(10)	20(4)
C(7)	3988(17)	7516(17)	4121(16)	29(5)
C(1)	2596(16)	4911(18)	1965(12)	21(5)
C(4)	2037(19)	6460(24)	3176(18)	56(9)
C(2)	1541(19)	5172(19)	2075(14)	30(6)
C(6)	4063(16)	6675(16)	3537(14)	14(5)
C(9)	5924(18)	7516(19)	4302(17)	36(6)
C(5)	3144(18)	6139(18)	3062(15)	29(6)
C(10)	5908(19)	6690(20)	3685(16)	34(6)
C(3)	1272(18)	5955(18)	2702(14)	29(6)
C(8)	4909(21)	7973(22)	4534(14)	42(7)

^{a} Equivalent isotropic U defined as one-third of the trace of the orthogonalized $\mathbf{U}_{ij}$ tensor.
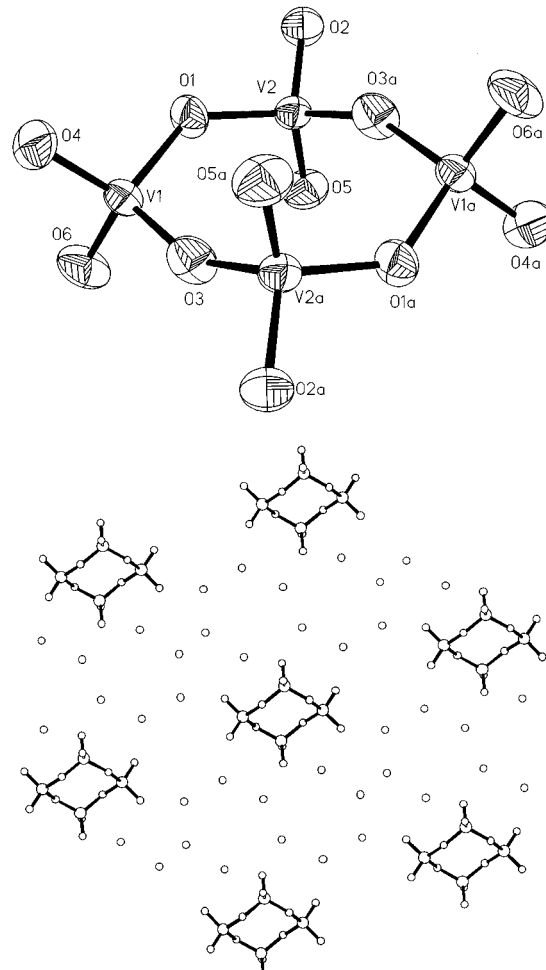
Figure 1. (a) Top: View of the structure of the anionic cluster of **1**, [V$_4$O$_{12}$]$^{4-}$. (b) Bottom: Virtual layer structure adopted in the structure of **1**·11H$_2$O.

solvents. Attempts to isolate the species from aqueous media under conventional conditions have proved fruitless. Similarly, attempts to isolate **1** under conventional conditions were unsuccessful. These observations reinforce the conclusion that the enhanced properties of solvent extraction of solids and crystal growth associated with the hydrothermal domain provide

Table 6. Selected Bond Distances (Å) and Angles (deg) for [Zn(bipy)$_3$]$_2$[V$_4$O$_{12}$]·11H$_2$O (**1**·11H$_2$O)

Distances			
Zn(1)−N(8)	2.195(8)	Zn(1)−N(9)	2.135(7)
Zn(1)−N(10)	2.147(8)	Zn(1)−N(11)	2.166(8)
Zn(1)−N(12)	2.134(7)	Zn(1)−N(13)	2.165(7)
V(1)−O(1)	1.804(6)	V(1)−O(4)	1.789(6)
V(1)−O(5)	1.631(7)	V(1)−O(11)	1.629(7)
V(2)−O(1)	1.777(6)	V(2)−O(3)	1.631(6)
V(2)−O(4)	1.793(7)	V(2)−O(6)	1.649(7)
O(1)−O(12)	2.74(1)	O(1)−O(10)	2.84(1)
O(2)−O(8)	2.77(1)	O(5)−O(7)	2.76(1)
O(6)−O(9)	2.75(1)	O(6)−O(10)	2.85(1)

Angles			
N(8)−Zn(1)−N(9)	76.4(3)	N(8)−Zn(1)−N(10)	166.6(3)
N(8)−Zn(1)−N(11)	94.0(3)	N(8)−Zn(1)−N(12)	92.3(3)
N(8)−Zn(1)−N(13)	94.6(3)	N(9)−Zn(1)−N(10)	95.2(3)
N(9)−Zn(1)−N(11)	93.5(3)	N(9)−Zn(1)−N(12)	165.8(3)
N(9)−Zn(1)−N(13)	95.8(3)	N(10)−Zn(1)−N(11)	75.9(3)
N(10)−Zn(1)−N(12)	97.5(3)	N(10)−Zn(1)−N(13)	96.7(3)
N(11)−Zn(1)−N(12)	95.8(3)	N(11)−Zn(1)−N(13)	168.6(3)
N(12)−Zn(1)−N(13)	76.3(3)	O(1)−V(1)−O(4)	110.9(3)
O(1)−V(1)−O(5)	108.2(3)	O(1)−V(1)−O(11)	110.7(3)
O(4)−V(1)−O(5)	109.8(4)	O(4)−V(1)−O(11)	109.2(3)
O(5)−V(1)−O(11)	108.0(4)	O(1)−V(2)−O(3)	109.8(3)
O(1)−V(2)−O(4)	107.6(3)	O(1)−V(2)−O(6)	111.6(3)
O(3)−V(2)−O(4)	108.8(3)	O(3)−V(2)−O(6)	109.3(4)
O(4)−V(2)−O(6)	109.7(3)	V(1)−O(1)−V(2)	136.0(4)
V(1)−O(4)−V(2)	154.5(4)		

Table 7. Selected Bond Distances (Å) and Angles (deg) for [{Zn(bipy)$_2$}$_2$V$_4$O$_{12}$] (**2**)

Distances			
Zn(1)−O(1)	2.075(3)	Zn(1)−O(1)	2.075(3)
Zn(1)−N(1)	2.226(3)	Zn(1)−N(1)	2.226(3)
Zn(1)−N(2)	2.078(3)	Zn(1)−N(2)	2.078(3)
V(1)−O(1)	1.639(3)	V(1)−O(2)	1.608(3)
V(1)−O(3)	1.800(3)	V(1)−O(3)	1.787(3)

Angles			
O(1)−Zn(1)−O(1)	96.9(2)	O(1)−Zn(1)−N(1)	85.6(1)
O(1)−Zn(1)−N(1)	170.8(1)	O(1)−Zn(1)−N(2)	94.8(1)
O(1)−Zn(1)−N(2)	94.9(1)	O(1)−Zn(1)−N(1)	170.8(1)
O(1)−Zn(1)−N(1)	85.6(1)	O(1)−Zn(1)−N(2)	94.9(1)
O(1)−Zn(1)−N(2)	94.8(1)	N(1)−Zn(1)−N(1)	93.4(2)
N(1)−Zn(1)−N(2)	76.0(1)	N(1)−Zn(1)−N(2)	93.9(1)
N(1)−Zn(1)−N(2)	93.9(1)	N(1)−Zn(1)−N(2)	76.0(1)
N(2)−Zn(1)−N(2)	165.4(2)	O(1)−V(1)−O(2)	109.5(2)
O(1)−V(1)−O(3)	108.6(1)	O(1)−V(1)−O(3)	110.0(1)
O(2)−V(1)−O(3)	108.3(1)	O(2)−V(1)−O(3)	108.7(2)
O(3)−V(1)−O(3)	111.7(1)	Zn(1)−O(1)−V(1)	148.0(2)
V(1)−O(3)−V(1)	136.9(2)		

Table 8. Selected Bond Lengths (Å) and Angles (deg) for [{Zn(o-phen)$_2$}$_2$V$_4$O$_{12}$]·H$_2$O (**3**·H$_2$O)

Distances			
Zn(1)−O(6)	2.065(3)	Zn(1)−O(18)	2.086(3)
Zn(1)−N(2)	2.165(4)	Zn(1)−N(3)	2.178(4)
Zn(1)−N(4)	2.166(4)	Zn(1)−N(5)	2.180(4)
Zn(2)−O(2)	2.064(3)	Zn(2)−O(13)	2.083(3)
Zn(2)−N(6)	2.161(4)	Zn(2)−N(7)	2.229(4)
Zn(2)−N(8)	2.218(4)	Zn(2)−N(9)	2.117(4)
V(1)−O(1)	1.623(3)	V(1)−O(11)	1.788(3)
V(1)−O(16)	1.781(3)	V(1)−O(18)	1.654(3)
V(2)−O(3)	1.799(3)	V(2)−O(7)	1.620(3)
V(2)−O(8)	1.781(3)	V(2)−O(13)	1.672(3)
V(3)−O(5)	1.614(3)	V(3)−O(6)	1.662(3)
V(3)−O(8)	1.789(3)	V(3)−O(11)	1.802(3)
V(4)−O(2)	1.658(3)	V(4)−O(3)	1.805(3)
V(4)−O(14)	1.615(3)	V(4)−O(16)	1.780(3)

Angles			
O(6)−Zn(1)−O(18)	92.6(1)	O(6)−Zn(1)−N(2)	91.3(1)
O(6)−Zn(1)−N(3)	97.0(1)	O(6)−Zn(1)−N(4)	167.2(1)
O(6)−Zn(1)−N(5)	91.7(1)	O(18)−Zn(1)−N(2)	92.7(1)
O(18)−Zn(1)−N(3)	165.6(1)	O(18)−Zn(1)−N(4)	84.0(1)
O(18)−Zn(1)−N(5)	98.7(1)	N(2)−Zn(1)−N(3)	76.4(1)
N(2)−Zn(1)−N(4)	101.1(1)	N(2)−Zn(1)−N(5)	168.0(1)
N(3)−Zn(1)−N(4)	88.8(1)	N(3)−Zn(1)−N(5)	91.8(1)
N(4)−Zn(1)−N(5)	76.7(1)	O(2)−Zn(2)−O(13)	92.4(1)
O(2)−Zn(2)−N(6)	94.9(1)	O(2)−Zn(2)−N(7)	85.8(1)
O(2)−Zn(2)−N(8)	170.2(1)	O(2)−Zn(2)−N(9)	95.5(1)
O(13)−Zn(2)−N(6)	94.6(1)	O(13)−Zn(2)−N(7)	170.3(1)
O(13)−Zn(2)−N(8)	94.6(1)	O(13)−Zn(2)−N(9)	97.6(1)
N(6)−Zn(2)−N(7)	76.1(1)	N(6)−Zn(2)−N(8)	91.3(1)
N(6)−Zn(2)−N(9)	163.6(1)	N(7)−Zn(2)−N(8)	88.4(1)
N(7)−Zn(2)−N(9)	92.1(1)	N(8)−Zn(2)−N(9)	76.8(1)
O(1)−V(1)−O(11)	110.0(2)	O(1)−V(1)−O(16)	108.9(2)
O(1)−V(1)−O(18)	109.5(2)	O(11)−V(1)−O(16)	110.2(2)
O(11)−V(1)−O(18)	108.3(2)	O(16)−V(1)−O(18)	109.9(2)
O(3)−V(2)−O(7)	109.3(2)	O(3)−V(2)−O(8)	110.0(2)
O(3)−V(2)−O(13)	107.5(2)	O(7)−V(2)−O(8)	109.5(2)
O(7)−V(2)−O(13)	109.0(2)	O(8)−V(2)−O(13)	111.5(2)
O(5)−V(3)−O(6)	109.8(2)	O(5)−V(3)−O(8)	110.6(2)
O(5)−V(3)−O(11)	107.5(2)	O(6)−V(3)−O(8)	111.5(2)
O(6)−V(3)−O(11)	108.0(1)	O(8)−V(3)−O(11)	109.2(3)
O(2)−V(4)−O(3)	108.2(2)	O(2)−V(4)−O(14)	108.5(2)
O(2)−V(4)−O(16)	110.3(2)	O(3)−V(4)−O(14)	109.8(2)
O(3)−V(4)−O(16)	110.4(2)	O(14)−V(4)−O(16)	109.5(2)
Zn(2)−O(2)−V(4)	132.8(2)	V(2)−O(3)−V(4)	123.3(2)
Zn(1)−O(6)−V(3)	136.0(2)	V(2)−O(8)−V(3)	144.6(2)
V(1)−O(11)−V(3)	124.5(2)	Zn(2)−O(13)−V(2)	137.3(2)
V(1)−O(16)−V(4)	157.1(2)	Zn(1)−O(18)−V(1)	133.5(2)

groups of adjacent vanadium sites is reminiscent of the structure of {[(η-C$_8$H$_{12}$)Ir]$_2$(V$_4$O$_{12}$)}$^{2-}$,[6] which also possesses the [V$_4$O$_{12}$]$^{4-}$ core but is covalently linked to [(η-C$_8$H$_{12}$)Ir]$^+$ fragments.

The structural parameters associated with the clusters of **1**−**3** are compared in Table 10. The metrical parameters for the structures are generally quite similar. The most notable exceptions are the parameters associated with bridging oxo groups. For both **1** and **3**, the V−O−V angles alternate within the ring, 136.0(4) and 154.5(4)° for **1** and 123.9(2) and 150.9(2)° for **3**. In contrast, the V−O−V angles for **2** are identical at 136.9(2)°, as a consequence of the crystallographically imposed symmetry. Likewise, the V−O−Zn angle of **2** is considerably more open than that associated with **3**, 148.0(2) vs 134.9(2)°, most likely as a consequence of the spanning of alternate vanadium sites in **2** rather than adjacent vanadium sites as observed for **3**.

That the chemistry of mixed metal oxide coordination clusters may be extended to the Mo/Ni/O system was demonstrated by the isolation of [{Ni(bipy)$_2$}$_2$Mo$_4$O$_{14}$] (**4**), whose structure is shown in Figure 5. The structure of **4** may be described as two {Mo$_2$O$_7$}$^{2-}$ units linked through two {Ni(bipy)$_2$}$^{2+}$ moieties

unique conditions for the preparation of materials, inaccessible by conventional synthetic methods.

The structure of **2**, shown in Figure 2, consists of isolated neutral hexanuclear clusters [{Zn(bipy)$_2$}$_2$V$_4$O$_{12}$]. In a fashion similar to the structure of the "naked" core [V$_4$O$_{12}$]$^{4-}$ associated with **1**, the core of **2** is the [V$_4$O$_{12}$]$^{4-}$ ring, which acts, however, as a bidentate "ligand" to each of two {Zn(bipy)$_2$}$^{2+}$ units. Each {Zn(bipy)$_2$}$^{2+}$ moiety bonds to two terminal oxo-groups, one from each of two alternate or cross-ring vanadium sites. Consequently, the {V$_4$O$_4$} ring of **2** possesses distinct curvature and boatlike configuration.

As shown in Figure 3, the structure of [{Zn(phen)$_2$}$_2$-V$_4$O$_{12}$]·H$_2$O (**3**) contrasts dramatically with that of **2**. While **3** shares the central [V$_4$O$_{12}$]$^{4-}$ structural motif with **2**, the covalently attached {Zn(phen)$_2$}$^{2+}$ moieties each bond to the terminal oxo groups of adjacent vanadium sites on the ring. This endows the cluster with a distinctly chairlike configuration. While the cluster of **2** possesses approximate C_{2h} symmetry, **3** exhibits approximate C_{2v} symmetry, as shown in Figure 4. The linking of the peripheral {Zn(phen)$_2$}$^{2+}$ fragments of **2** to oxo

Table 9. Selected Bond Lengths (Å) and Angles (deg) for [{Ni(bipy)$_2$}$_2$Mo$_4$O$_{14}$] (**4**)

Mo(1)−O(1)	1.705(15)	Mo(1)−O(2)	1.753(17)
Mo(I)−O(4)	1.741(15)	Mo(1)−O(3A)	1.874(4)
Ni(2)−O(4)	2.091(15)	Ni(2)−N(1)	2.047(15)
Ni(2)−N(2)	2.074(16)	Ni(2)−O(4A)	2.091(15)
Ni(2)−N(1A)	2.047(15)	Ni(2)−N(2A)	2.074(16)
O(3)−Mo(1A)	1.874(4)	O(3)−Mo(1B)	1.874(4)
N(1)−C(1)	1.353(25)	N(1)−C(5)	1.330(27)
N(2)−C(6)	1.387(27)	N(2)−C(10)	1.310(29)
C(7)−C(6)	1.356(30)	C(7)−C(8)	1.408(34)
C(1)−C(2)	1.349(31)	C(4)−C(5)	1.430(37)
C(4)−C(3)	1.331(36)	C(2)−C(3)	1.384(31)
C(6)−C(5)	1.489(30)	C(9)−C(10)	1.372(34)
C(9)−C(8)	1.415(35)		
O(1)−Mo(1)−O(2)	111.1(8)	O(1)−Mo(1)−O(4)	107.5(7)
O(2)−Mo(1)−O(4)	109.1(7)	O(1)−Mo(1)−O(3A)	110.3(5)
O(2)−Mo(1)−O(3A)	107.7(8)	O(4)−Mo(1)−O(3A)	111.3(8)
O(4)−Ni(2)−N(1)	92.2(6)	O(4)−Ni(2)−N(2)	171.0(7)
N(1)−Ni(2)−N(2)	79.6(7)	O(4)−Ni(2)−O(4A)	87.7(8)
N(1)−Ni(2)−O(4A)	93.4(6)	N(2)−Ni(2)−O(4A)	89.2(6)
O(4)−Ni(2)−N(1A)	93.4(6)	N(1)−Ni(2)−N(1A)	172.2(9)
N(2)−Ni(2)−N(1A)	95.1(7)	O(4A)−Ni(2)−N(1A)	92.2(6)
O(4)−Ni(2)−N(2A)	89.2(6)	N(1)−Ni(2)−N(2A)	95.1(7)
N(2)−Ni(2)−N(2A)	95.2(9)	O(4A)−Ni(2)−N(2A)	171.0(7)
N(1A)−Ni(2)−N(2A)	79.6(7)	Mo(1A)−O(3)−Mo(1B)	160.7(13)
Mo(1)−O(4)−Ni(2)	136.7(8)		
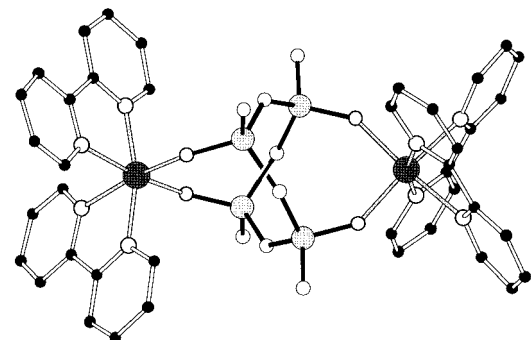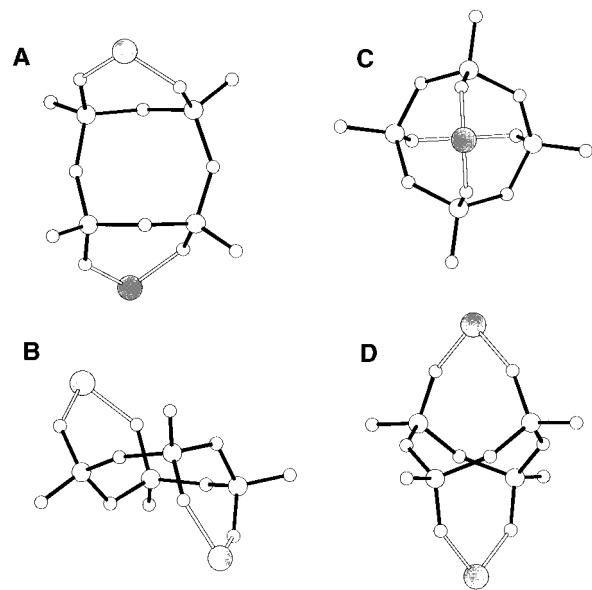
Figure 2. View of the structure of [{Zn(bipy)$_2$}$_2$V$_4$O$_{12}$] (**2**).
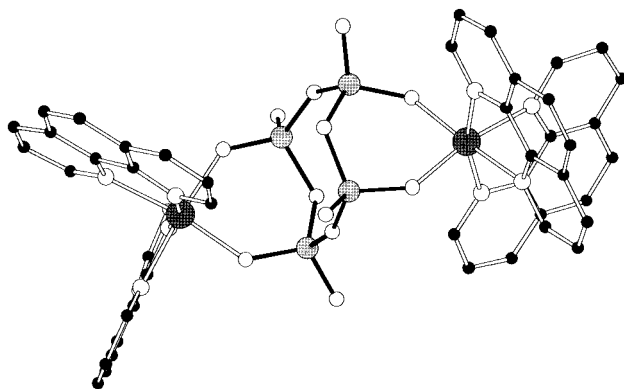
Figure 3. View of the structure of [{Zn(o-phen)$_2$}$_2$V$_4$O$_{12}$] (**3**).

into a 12-member {Mo$_4$Ni$_2$O$_6$} ring structure. The dimolybdate units of **4** are structurally related to the dimolybdate anion [Mo$_2$O$_7$]$^{2-}$ which has been isolated as the tetrabutylammonium salt.[29] While [Mo$_2$O$_7$]$^{2-}$ is stable in nonaqueous solvents in the presence of large organic counterions with respect to polycondensation, the anion cluster cannot be isolated from aqueous molybdate solutions under conventional conditions.

On the other hand, the analogous anion (Cr$_2$O$_7$)$^{2-}$ is ubiquitous. The structure of [{Mn(bipy)$_2$}$_2$Cr$_4$O$_{14}$]$^{2+}$ [30] consists
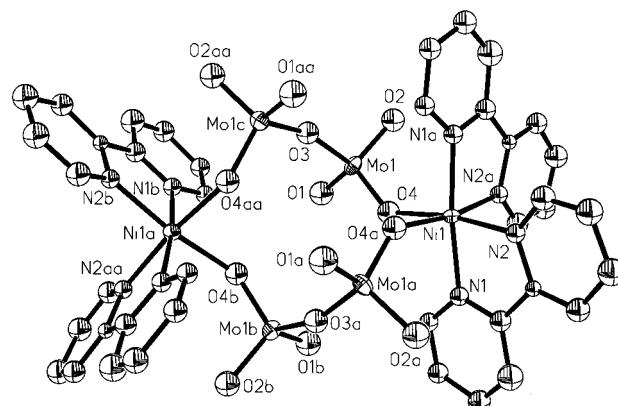
(29) Day, V. W.; Fredrich, M. F.; Klemperer, W. G.; Shum, W. *J. Am. Chem. Soc.* **1977**, *99*, 6146.

(30) Dave, B. C.; Czernuszewicz, R. C. *Inorg. Chem.* **1994**, *33*, 847.

Figure 4. Comparison of the cluster cores of **2** and **3**.

Table 10. A Comparison of the Metrical Parameters (Å, deg) of the Structures of **1**−**4**[a]

	1·11H$_2$O	**2**	**3·H$_2$O**	**4**	
Zn−N	2.157(9)	2.078(3)	2.156(4)	2.05(2)	Ni−N
		2.226(3)	2.198(5)	2.08(2)	
Zn−O		2.075(3)	2.075(3)	2.08(2)	Ni−O
V−O$_t$	1.635(9)	1.608(3)	1.618(4)	1.74(2)	Mo−O$_t$
V−O$_b$(V)	1.791(9)	1.794(4)	1.791(4)	1.876(4)	Mo−O$_b$(Mo)
V−O$_b$(Zn)		1.639(3)	1.662(4)	1.74(2)	Mo−O$_b$(Ni)
O−V−O	109.5(4)	109.5(2)	109.5(3)	109.5(9)	O−Mo−O
V−O−V	136.0(4)	136.9(2)	123.9(2)	160.2(12)	Mo−O−Mo
	154.5(4)		150.9(2)		
V−O−Zn		148.0(2)	134.9(2)	137.5(9)	Mo−O−Ni
O−Zn−O		96.9(2)	92.5(1)	86.9(9)	O−Ni−O

[a] Entries under 4 refer to the interactions listed on the righthand side column.

Figure 5. Structure of the heterometallic hexanuclear cluster [{Ni(bipy)$_2$}$_2$Mo$_4$O$_{14}$] (**4**).

of two dichromate units linked by two {Mn(bipy)$_2$}$^{2+}$ groups to give a {Mn$_2$Cr$_4$O$_6$} ring analogous to the {Ni$_2$Mo$_4$O$_6$} ring of **4**.

The geometry about the molybdenum sites of **4** is distorted tetrahedral, defined by an oxo group bridging the two Mo centers, two terminal oxo groups, and an oxo group bridging the Mo and Ni sites. The Ni coordination geometry is distorted octahedral {NiN$_4$O$_2$} with the oxygen donors in the *cis* orientation. The metrical parameters for the Mo and Ni sites are unexceptional.

Conclusions

While it is now apparent that numerous metastable oxometalate solid phases may be prepared by hydrothermal methods,[31] the isolation of **1**−**4** demonstrates that there are domains in the hydrothermal parameter space which favor the isolation of molecular species of unusual structures and nuclearities. The covalent attachment of coordination complex fragments to oxometalate cores in **2**−**4** suggests that such structures may be a common feature of certain hydrothermal domains. Not only the molecular species of this study but chain and layered structures based on metal oxide clusters with peripheral coordination complex moieties have now been described. The application of principles derived from the coordination chemistry of classical complexes to the synthesis of complex clusters and even solid phases appears to provide a low-temperature approach to the development of new materials whose properties may be modified by judicious choices of components.

(31) Stein, A. J.; Keller, S. W.; Mallouk, T. E. *Science* **1993**, *259*, 1558.